*Sensors and Materials*, Vol. 30, No. 8 (2018) 1655–1664
MYU Tokyo

S & M 1622


# Flexible Force-sensing System for Wearable Exoskeleton Using Liquid Pressure Detection

Yanhe Zhu,* Guoan Zhang, Weiming Xu, and Jie Zhao

State Key Laboratory of Robotics Institute, Harbin Institute of Technology University,
HIT University Science Park Robotics Institute 203, Building C1, Room 203, Science Square, Yikuang Street No. 2,
Nangang District, Harbin, Heilongjiang Province 150006, China

(Received March 14, 2017; accepted March 5, 2018)

***Keywords:*** gait monitoring, liquid pressure, plantar pressure distribution, rehabilitation exoskeleton

A gait monitoring system based on liquid pressure detection was designed. In this work, based on the study of the plantar pressure distribution, a special cylindrical liquid cavity was located under the foot. For the actual application of an exoskeleton, the human foot is curved by uneven terrain in the alternation of the support and swinging phases. To measure the pressure distribution of the sole over a large measurement range, shoes also need to be flexible. By measuring the fluid pressure, the plantar pressure distribution can be detected during human walking. Assuming sufficient flexibility, this approach could ensure the stable measurement on uneven terrain for the exoskeleton.

## 1. Introduction

With the development of social science and technology, much attention has been paid to power-assistant robots that can help people walk or carry heavy things. With the advantages of closely connecting humans and machines, exoskeleton robots have become a target for development. In an exoskeleton controlling system, the human is the controlling center. An exoskeleton controller can detect the intent of the motion and control the corresponding parts of the drive module by sensors. At the same time, the comparison between the human body and the exoskeleton motion is analyzed to provide feedback to ensure that the exoskeleton can respond to human action quickly and accurately. Therefore, the detection of human gait is a very important part of an exoskeleton control system. It directly affects the assistant effect on the human body. By arranging sole force sensors, the distribution of plantar pressure loads of movement can be detected and the current human walking gait can be identified.

From the beginning of the 1990s, electronics and the sensor technology for the measurement of plantar pressure have been greatly improved, and force-electric conversion technology has been widely studied and applied.(1,2) At Monash University, Darwin(3) utilized piezoresistance to design a force testing platform, in which 144 piezoresistances had been distributed to provide a greater area for motion. Srinivasan in British used a similar approach for a multimodule

*Corresponding author: e-mail: yhzhu@hit.edu.cn
http://dx.doi.org/10.18494/SAM.2018.1875

ISSN 0914-4935 

stress test plate, which enabled the arrangement of a sensing array on a large scale. The integration density of piezoresistances was up to 4032/cm$^2$. Morris[4] designed shoes for use in force measurements. He placed a polyvinylidene fluoride (PVDF) piezoelectric film and the piezoresistance in the toe and heel, from which the plantar pressure distribution could be obtained.[5]

As for the exoskeleton, Harvard[6,7] designed a flexible sensor using the technique of measuring the change in liquid metal resistance to realize three-dimensional (3D) force measurements. Because of its small contact area and limited range (10 N), it is mainly used in the measurement of man–machine contact force. Kazerooni studied a gas pressure sensor with gait detection, which could detect the patient's gait to carry out a diagnosis. Because of the minimal stiffness of the gas, it is not suitable for measuring exoskeleton gait. The university of Berkeley BLEEX[8,9] exoskeleton robot also adopted a liquid pressure testing method to measure plantar pressure, as well as a foot switch auxiliary support and a swing phase switch at the bottom of the shoes.[10–13] However, it measured a foot in the form of an outline around the total pressure, which did not realize a distributed measurement.

For an exoskeleton robot, the accuracy of the sensor is generally required. However, the feet of the human and shoes of the exoskeleton need to be fitted well. This requires that exoskeleton shoes have good flexibility and can overcome the situation in which the trends and state of movement need to be detected on uneven terrain.[14] Currently, most flexible sensors can accurately measure the force, but on uneven surfaces, damage may occur at all probabilities. This study mainly uses the liquid pressure distribution measurement method to detect plantar pressure by changing the outer wall features of the fluid cavity. Although it can achieve general accuracy, this method ensures the linearity and repeatability of measurements on both flat and curved surfaces, and the shoes can accommodate the shear force under the premise that they have good flexibility. Thereby, it can be used in the exoskeleton and improve the stability of the gait monitoring system.

## 2. Design of Flexible Liquid Cavity

### 2.1 Analysis of plantar pressure

Level-walking research is the foundation for the mechanic analysis of human lower limb movement. In the course of walking, both feet alternately contact and separate from the ground, and the foot contact is a rolling process. In the walking cycle, the single-leg-stance phase ranges from 80 to 90%, and the double-leg-stance phase ranges from 10 to 20%.

In the analysis of a single leg, a complete gait cycle consists of stance and swing phases. The stance phase includes the double-and single-foot-stance phases. In the complete gait cycle, the double-foot-stance phase accounts for 20%, the single-foot-stance phase accounts for 40%, and the swing phase accounts for 40%.

The plantar pressure trend in a normal human gait cycle is shown in Fig. 1.[15,16] Plantar pressure is distributed over four points: one in the heel, two in the forefoot, and one in the big toe. At the beginning of the initial contact, the stress is concentrated at the heel. With the

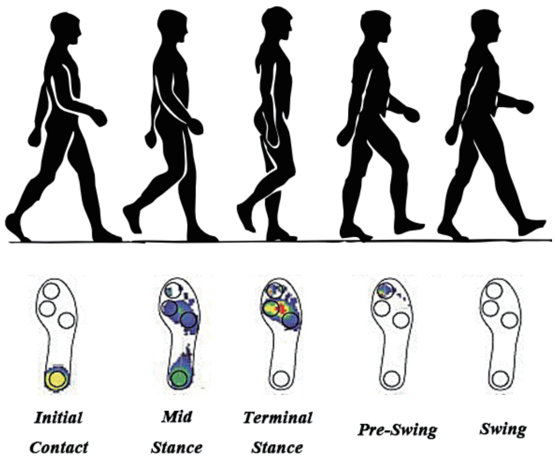


Fig. 1. (Color online) Trends in plantar pressure in the normal gait cycle.

body center of gravity moving forward, the pressure is slowly transferred to the forefoot; at the midstance, the pressure is substantially uniformly distributed around the foot; at the terminal stance, the center of gravity continues to move forward along with the heel pressure and gradually decreases to zero. Otherwise, the forefoot pressure increases and enters the swing phase. In the pre-swing phase, only the big toe retains the pressure, and in the swing phase, the pressure decreases to 0.

In a gait cycle, there are significant differences in the plantar pressure distribution. In the same phase, during the different stages, the plantar pressure distribution also displays significant differences. Thus, observing the trend of foot pressure is a simple and effective method of detecting the gait cycle.

### 2.2 Materials and methods

Considering the environment of the exoskeleton, this study uses a liquid chamber as a unit to measure the plantar pressure. Compared with other methods, the technique of hydraulic pressure measurement can convert surface pressure into a uniform pressure within the liquid accurately, and have a greater compression rigidity and flexibility.

Figure 2 is a theoretical model of the liquid cavity. The upper and lower surfaces of the cavity are a high-rigidity plate, and the side wall of the cavity is a material with small elastic deformation that can be bent and folded. The cavity is filled with liquid and achieves its maximum volume when the side wall is formed into a hemisphere. At that time, any force exerted on the surface of the cavity leads to the compression of the volume of liquid, while a change in the force on the upper surface leads to a change in the internal liquid pressure.

Based on this theory, silica gel is used as the main material to display different degrees of hardness. The structure is shown in Fig. 3. Section labeled 4 is the liquid cavity. To ensure that the liquid is at its maximum volume, the side wall labeled 3 is set in a hemisphere. In Fig. 3, sections labeled 1, 3, and 5 are formed by injection molding of Silicone 70. The thickness of section 3 is 0.5 mm to guarantee the physical characteristics in the sidewall. Section 2 is

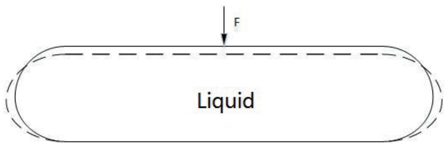


Fig. 2. Theoretical model of the liquid cavity.

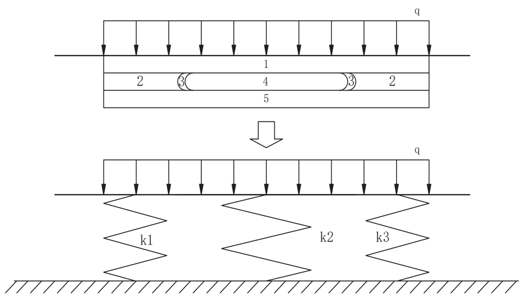


Fig. 3. Schematic diagram of the measurement.

injection-molded using Silicone 0, and owing to its small hardness, it can be regarded as a material that can be compressed easily.

Because section 3 is a thin wall that is easily bent and deformed, it is equivalent to a small rigid spring. Because liquids cannot be compressed easily, it can be equivalent to a spring with high stiffness. Therefore, the overall structure is equivalent to the spring model shown in the lower part of Fig. 3. The terms k1, k2, and k3 represent the stiffness of each part. When $q$, which is a uniformly distributed load, acts on the measuring unit, the major supporting force is provided by k2. The force generated by k1 and k2 and that generated by k3 are not within an order of magnitude, so the force generated by k1 and k3 is negligible. In this manner, the load can be converted into hydraulic pressure.

## 3. Overall Design of Force-sensing Shoes

### 3.1 Design of insole

For the gait described in the previous section, the analysis can be drawn during level-walking. Plantar pressure is mainly distributed over four points: two in the forefoot, one in the heel, and one in the big toe. However, the lower extremity exoskeleton does not set drives in the toe area. When a person wears the robot, the walking mode changes slightly. Operators skip the pre-swing phase and go directly into the swing phase. Therefore, to determine the situation with a human gait, three points are selected in this design: two in the forefoot and one in the heel.

The final design of the force-measuring insole is shown in Figs. 4 and 5. The insole is divided into three layers, and the thickness of each layer is 3 mm. The upper and lower layers are made from Silicone 70. Mesosphere layers are made from Silicone 0. Mesosphere layers have three cavities at force nodes. Cavity sidewalls are annular rings in Silicone 70, and the surfaces of the annular rings are hemispherical. A Flexiforce A301 force-sensing register (FSR) is used as the measuring sensor. To prevent conductivity, oil is selected to fill the cavity. The FSR is placed in oil and used for the real-time measurement of the oil pressure.

When a human stands on the force-measuring insoles, the force is passed to the ground primarily through three oil cavities. At this time, the human gait can be determined by collecting the FSR resistance signal of the oil cavity. Because the material is silica gel, the

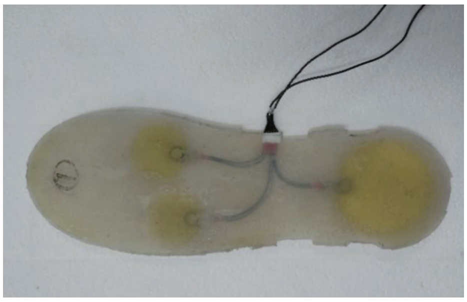

Fig. 4. (Color online) Physical diagram of the insole.

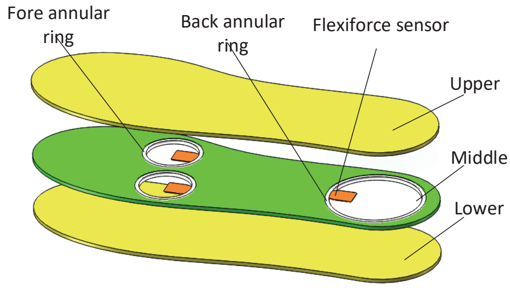


Fig. 5. (Color online ) Structure of the insole.

overall structure has good flexibility. The consistency between force measuring insoles and shapes of the human foot in motion can be guaranteed; as a result, human–machine coordination has been optimized.

### 3.2 Design of the sole

The sole is designed primarily to solve problems of connection with the exoskeleton. This design avoids direct contact between force-measuring insoles and the ground, improving the stability of the overall structure as well. The contact switch sensor is set under the sole and parallel to the force-measuring insoles on the circuit. Because, in practice, the reaction of the force-measuring insoles is a continuous signal, if interference and accidental errors occur, they will have a huge negative impact on the overall control. Therefore, the contact switch sensor can increase the accuracy of differentiation between the support phase and the swing phase, and improve control stability.

The design principle of the contact switch sensor is shown in Fig. 6. Rubber is used to build the cavity, and electrodes are attached to the upper and lower surfaces of the cavity. When the soles touch the ground and enter into the support phase, the lower surface deforms, causing the electrodes to short and put out a low-resistance signal. When the soles leave the ground and enter into the swing phase, because of rubber elasticity, the surface moves back into shape and the electrodes are disconnected.

Figure 7 is a pictorial diagram of the contact switch sensor. There are six grooves in the rubber pad that are used for receiving metal electrodes. Six metal electrodes are arranged in parallel, constituting the contact switch with the copper foil under the rubber soles. If any point is touched, the line is turned on, and the real-time ground information is passed to a host computer, assisting the gait analysis.

A pictorial diagram of the force-sensing shoes is shown in Fig. 8. Force-sensing shoes are divided into four parts: force-measuring insoles, metal connectors, rubber soles, and contact switch sensors. Force-measuring insoles are at the top part of the shoes touching the human feet, measuring the force between the robot and human feet; the middle of the shoe consists of metal connectors and rubber soles, providing a machine connection with the flange of the exoskeleton and the entire support. The lower part of the shoes is the contact switch sensor, which detects the touchdown state.

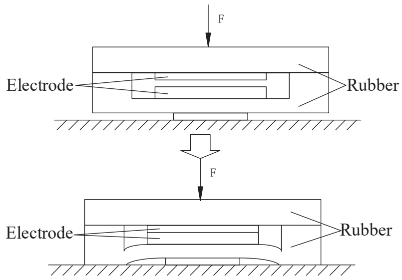


Fig. 6. Schematic diagram of contact switch sensor.

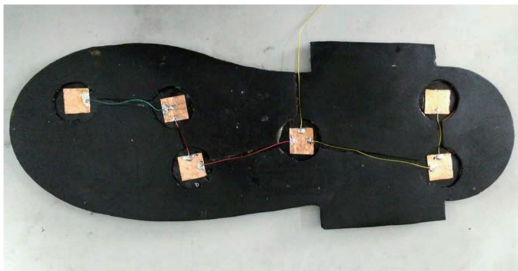

Fig. 7. (Color online) Physical diagram of contact switch sensor.

Fig. 8. (Color online) Overall structure of force-sensing shoes.

## 4. Experiments

### 4.1 Experiment of the single cavity

According to the experiment with the liquid cavity in a plane, a curve, and a bevel (anti-shearing ability), the load capacity of the insole can be confirmed in different environments. Figure 9 shows a performance test of the force-measuring insole.

Acquired by the circuit board, the change in the resistance of the FSR is transformed into a voltage change and recorded in the form of a graph on the computer. The experiment involves gradual loading on the cylinder unit, and a horizontal ruler is used to ensure the level of the load. Because silica gel has a certain elasticity, when the mass was less than 10 kg, the measured values did not change regularity. The starting node was 4 kg and the incremental steps were 2 kg until the load reached 76 kg. We collect 15 sets of data at each node. The resulting data are plotted in Fig. 10.

Single-point experiments mainly verify the linear relationship between the loading and the voltage, and test the repeat accuracy and anti-cutting ability of the fluid cavity on the curved plane. Although the accuracy in the measurement is typical, the cylindrical force-measuring unit has certain degrees of linearity and repeatability. In the gait detection of exoskeletons, the identification of movement in different environments needs to be realized.

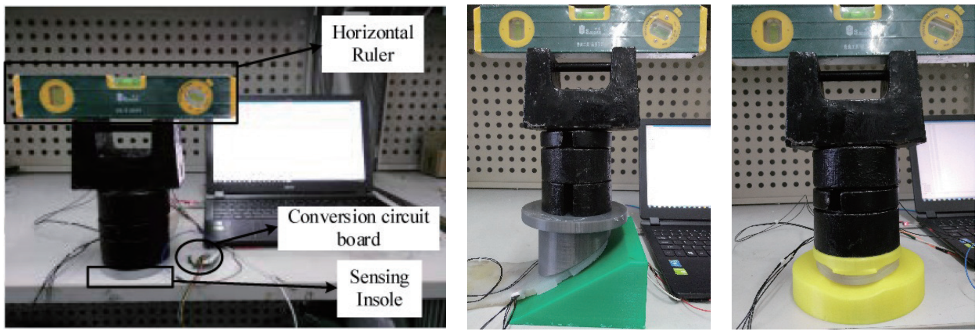


(a) (b) (c)

Fig. 9. (Color online) Single-point test platform: (a) plane loading test, (b) bevel loading test, and (c) curve loading test.

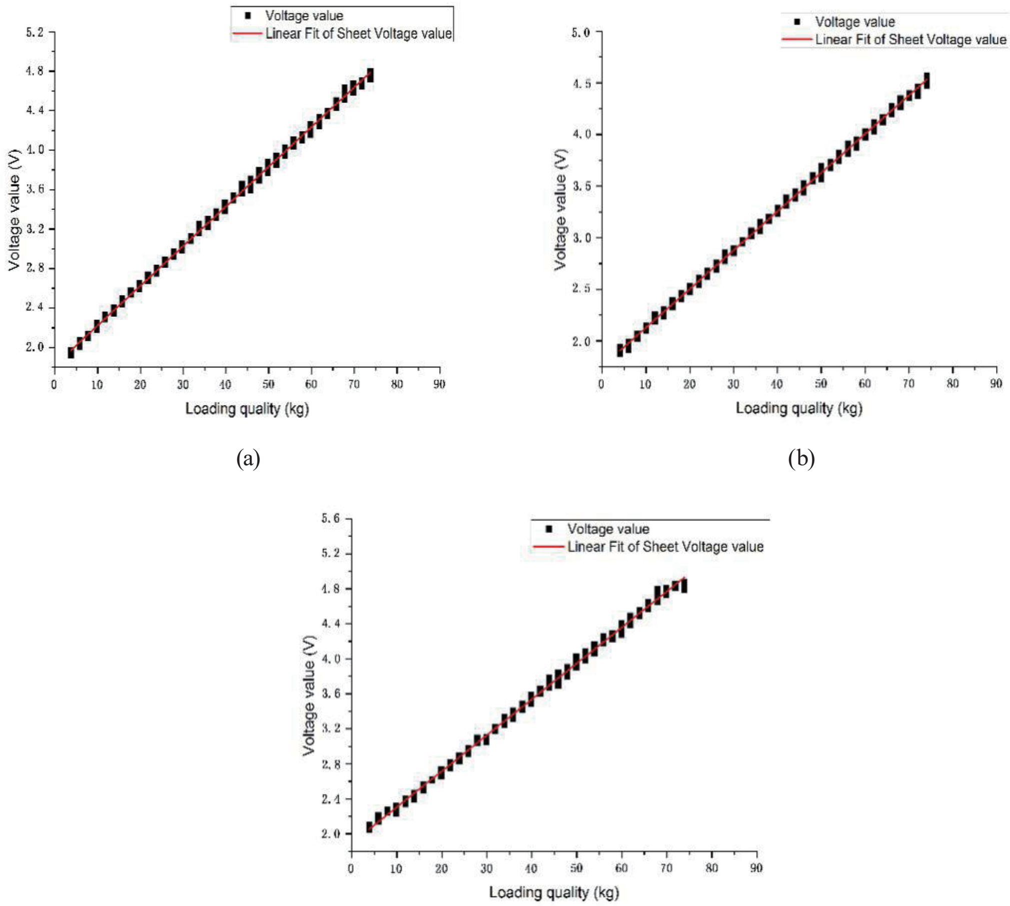


(c)

Fig. 10. (Color online) Single-point test data diagram. (a) Plane loading data. The black box is the result of 15 measurements. In a flat environment, the liquid cavity reflects an increasing trend and has good repeatability. (b) Bevel loading data. Under the effect of shearing forces, the liquid cavity still has good linearity and repeatability, indicating that the liquid cavity has the ability to resist shearing forces. From the numerical point of view, the value in the bevel protocol is lower than that in the plane protocol, because the force component of the friction is generated, causing the overall value to decrease. (c) Curve loading data. According to the data in the curve text, the liquid cavity still guarantees repeatability in the curved plane. The overall value has increased, because the contact area in the direction of gravity is reduced, resulting in a pressure increase compared with that in the case of the the plane.

### 4.2 Experiments

In this experiment, the researcher weighted 60 kg, put on the force-sensing shoes, and then began the level-walking and running protocol. Curves are shown in Figs. 11 and 12.

Through the analysis of Fig. 11, it can be concluded that in level-walking, the force is transmitted from the back to the front, at the same time representing the direction of movement in the body's center of gravity. Owing to inertial force in level-walking, the force increases significantly when the foot touches the ground and leaves the ground. This increasing trend may provide the basis for distinguishing motion.

Figure 12 shows that there are two obviously different points compared with the level-walk curve. First is the existence of the double-foot-swing phase. Second is that the curve slopes more severely during foot contact with the ground and when the foot leaves the ground.

According to the features of the curve, the distinction between walking and running can be made. In the initial stage, a person's movement can be clearly distinguished by detecting the rising speed of the force. If the rising speed is fast, people begin to run. A low rising speed indicates that people are walking. On the foot landing stage, a person's movement can be distinguished by detecting whether the feet contact the ground. When the single foot stance phase come to an end, the condition goes into the double foot stance phase, indicating that the state is walking. After the single foot stance phase, the condition directly changes into the double-foot-swing phase, indicating that the person is running.

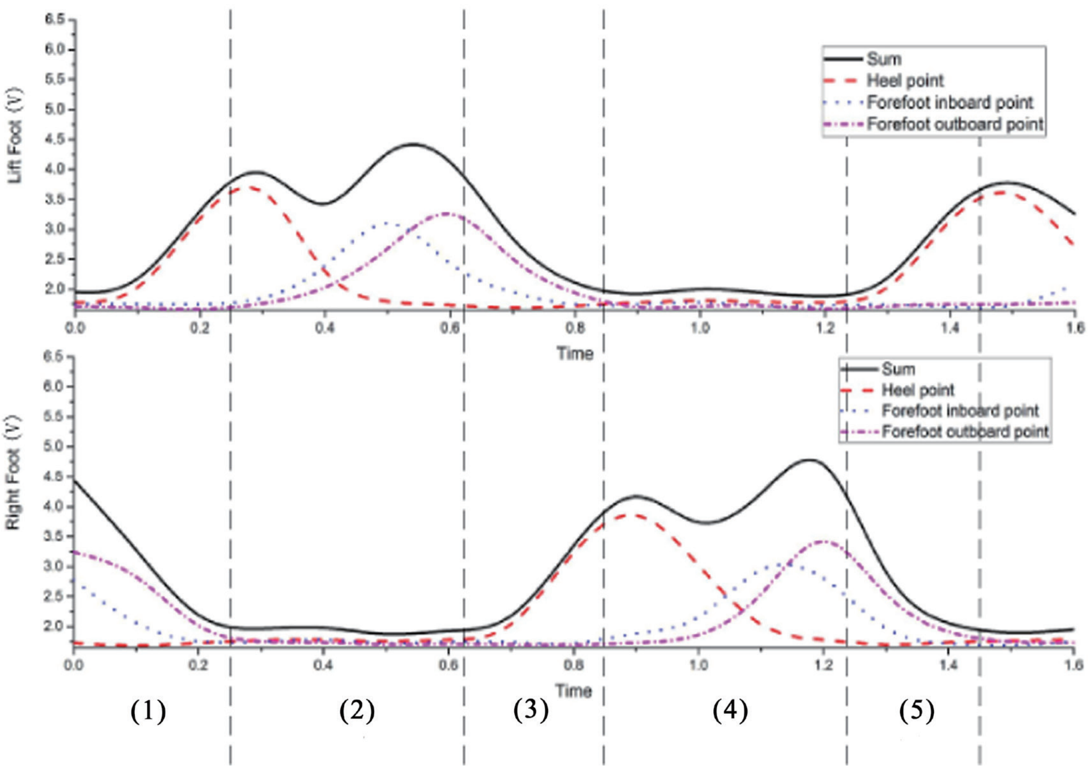


Fig. 11. (Color online) Level-walk curve. The left foot is taken as an example. (1) Double foot stance phase. (2) Single foot stance. (3) Double foot stance phase. (4) Swing phase. (5) Double foot stance phase.

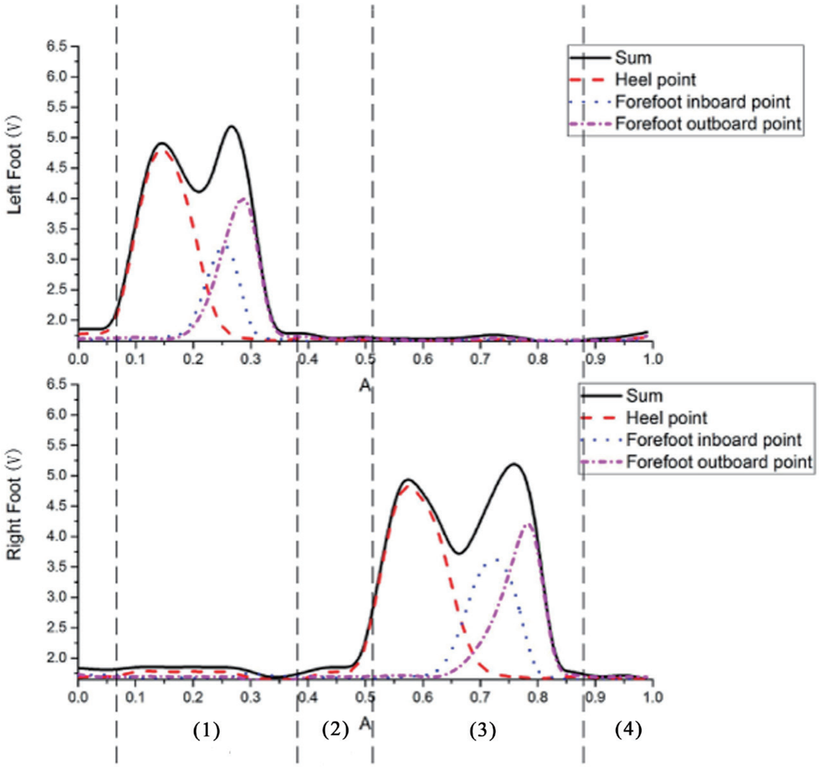


Fig. 12. (Color online) Running curve. The left foot is taken as an example. (1) Single foot stance. (2) Double foot swing phase. (3) Single foot stance. (4) Double foot swing phase.

## 4. Discussion and Conclusion

The structure of flexible force-sensing shoes for a rehabilitation exoskeleton is designed by liquid pressure detection. In this study, to enable stable measurement, in uneven terrain by the exoskeleton, the use of a liquid cylindrical cavity is introduced to obtain the plantar pressure distribution. By changing the structure of the cylindrical cavity, the stability of the measurements is guaranteed, and a contact switch is set up to comply with the structure of the soles of the feet to perfect the designing of the foot of the exoskeleton. Experimental data collection from the bottom of the feet proved the feasibility of the theory in this study. In future work, we will improve the reliability of the mechanical structure, raise the accuracy of the measurement of running, and finish the design work for docking the electrical and control systems of the exoskeleton.

## Acknowledgments

The work reported in this paper is funded by the National Key Research and Development Program (Grant: 2016YFC0800607) and the National Nature Science Foundation of China (U1613219).

## References


1 N. Wettels, V. J. Santos, R. S. Johansson, and G. E. Loeb: Adv. Rob. **8** (2008) 829.
2 R. D. P. Wong, J. D. Ponce, and V. D. Santos: Sens. Actuators, A **179** (2012) 62.
3 S. M. N. A. and D. Gouwanda: Proc. World Academy of Science Engineering & Technology (2011) 78.
4 S. J. Morris and J. A. Paradiso: Massachusetts Institute of Technology **3** (2004) 2468.
5 K. N. Bachus, A. L. Demarco, and K. T.Judd: Med. Eng. Phys. **28** (2006) 483.
6 D. Vogt, Y. L. Park, and R. J. Wood: Proc. IEEE Sensors 2012 Conf. (2012) 897.
7 Y. L. Park, B. R. Chen, and R. J. Wood: IEEE Sens. J. **12** (2012) 2711.
8 H. Kazerooni, R. Steger, and L. Huang: Int. J. Rob. Res. **25** (2006) 561.
9 H. Kazerooni and A. Chu: IEEE/ASME Trans. Mechatron. **11** (2006) 128.
10 H. Kazerooni, J. L. Racine, and L. Huang: Conf. Robotics and Automation (2006) 4353.
11 A. Chu, H. Kazerooni, and A. Zoss: Conf. Robotics and Automation (2005) 4345.
12 A. Zoss, H. Kazerooni, and A. Chu: 2005 IEEE/RSJ Int. Conf. (2005) 3465.
13 A. Zoss and H. Kazerooni: Adv. Rob. **20** (2006) 967.
14 Y. Long, Z.-J. Du, W.-D. Wang, G.-Y. Zhao, G.-Q. Xu, L. He, X.-W. Mao, and W. Dong: Sensors **16** (2016) 1408.
15 J. A. García-Calzón and M. E. Díaz-García: Sens. Actuators, B **123** (2007) 1180.
16 R. S. Dahiya, P. Mittendorfer, and M. Valle: IEEE Sens. J. **13** (2013) 4121.